

Flutter Analysis of Supersonic Wing with External Stores

Nur Azam Abdullah¹, Erwin Sulaeman²

¹ Department of Mechanical Engineering
International Islamic University Malaysia
Kuala Lumpur, Malaysia

¹ mokar_cafe@yahoo.com, ² esulaeman@iium.edu.my

ABSTRACT

One of the most dangerous aeroelastic failure phenomenon is flutter. The flutter characteristic is different for each type of aircraft depends on the wing geometry and its operational region of subsonic, transonic or supersonic. Prior to performing flight flutter test, extensive numerical simulations and Ground Vibration Test should be conducted where the structural finite element modes and the experimentation results should be matched otherwise the numerical simulation model could be rejected. In the present paper, the simulation of supersonic wing equipped with external loads of missiles on the wing had been analyzed at high supersonic region. The structural mode shapes at each generated frequency mode are also visually presented. The analysis is carried out using FEM software of MSC Nastran. The wing flutter with the external stores had been simulated at different altitudes. The result shows that the flutter velocity is sensitive to the flight altitude. For this reason, the flutter analysis is conducted also for a negative altitude. The negative altitude is obtained by considering the constant equivalent speed-Mach number rule at flutter speed boundary as a requirement in standard regulation of transport aircraft.

Keywords- Aeroelasticity, flutter, finite element method, external store, mode shape.

1. INTRODUCTION

Aeroelasticity can be defined as a branch of aeromechanics that deals with the interaction among inertial, aerodynamic and structural stiffness effects in air vehicle design [1]. Flutter is one of the aeroelasticity instability problem in which the structure model extracts energy from the air stream and unstably self-excited causes in catastrophic structural failure.

There are several types of basis mathematical model of aircraft in aeroelasticity which are Stiffness model-“Beam-Like” representation, Stiffness model-“Box Like” representation, Stiffness model-“Box Like Condensed to a Beam Like” model, and Mass model, Modal model, Damping model, and Rigid Aircraft model for testing or simulation [2]. In this paper, the presentation of the model used for the wing structure is the “Box Like” representation where structural detail is explored and analyzed accordingly. The present flutter analysis is conducted based on certification standards for military fighter aircraft such as MIL-A-8861[3] which put the aeroelastic requirement under Subpart 3: Construction, Material and Design and MIL-A-8870 at Section 6.4 [4]. To determine the sizing of wing structure, a maximum aerodynamic load distribution during pitch up maneuver is assumed and a finite element approach has been used to set up the structural stiffness for the wing by recognizing its detailed ‘box like’ construction. The present wing structure data should be validated further by comparing to Ground Vibration Test

(GVT) result where the main frequencies and mode shapes of the numerical model should be in agreement with the GVT results [5].

External stores can be defined as any objects such as missiles, gun and fuel tank which attached to the wing outside the wing box model. Since the stores attached to the wing, the missile launcher is designed based on the missiles weight and there should be a clearance of at least 8 cm if the missiles are mounted near to each other [6]. Each external store center of gravity must be placed as far forward as possible with respect to the elastic axis to delay the occurrence of flutter, while satisfying other design constraints [7]. For this paper, the analysis is performed in supersonic flow in which the external stores attached to the wing are two types of missiles and performed variation in altitude. The technical data for the missile were taken from [8] and [9].

The aeroelastic simulation model used in the present work consists of two parts: structural model and aerodynamic model. The structural model of the wing box skin is based on a quadrilateral shell element, while the external store and launcher are bar elements. The analysis takes into account the in-plane membrane characteristics as well as lateral bending and shear of the shell element. The material used for the wing box is Aluminum which is used as a base line data for future work where the wing box skin is designed as composite structure.

The aerodynamic model of the wing for supersonic region is based on boundary element method where the unsteady aerodynamics model of ZONA51 method of MSC Nastran [10] is used. For the subsonic region, the doublet lattice method of MSC Nastran is used. Note that, even though the present wing is designed for supersonic region, the flutter analysis is required to perform at subsonic region to ensure the instability does not occur in the flight design envelope. To ensure compatibility between the structural finite element and boundary element models a surface spline such that the 6 degrees of freedom structural deformations at each point is related to the aerodynamic deformations at each aerodynamic trapezoidal panel.

There are several methods to analyze the flutter speed based on the frequency matching such as K method and PK method [10, 14]. This paper presents the flutter speed results using PK Method [10]. Based on [2], the PK-Method is used to determine the aerodynamics stiffness and damping matrices using the reduced frequency.

SOL 103 of MSC Nastran is used to simulate the normal modes of each frequency. SOL 145 of MSC Nastran is utilized to obtain the damping and reduced frequency variation along the velocity. From this SOL 145 the flutter speed can be determined when the graph of velocity versus damping factor is plotted. This paper presents the first 10 fundamental normal modes of SOL 103 and determines the flutter speed of this supersonic wing with external stores by considering the variation of altitudes.

2. STRUCTURAL ANALYSIS

2.1. Supersonic Wing Characteristic

The present work utilizes a wing planform with an aspect ratio of 5 and taper ratio of 0.5. The wing swept back angle is 25°. The airfoil of this supersonic wing is a double wedge shape as shown in Fig. 1. The wedge angle of the airfoil is 10°. Along the wing span, the airfoil is divided into three parts which are main wing box and two control surfaces at leading edge and trailing edge. The portions of the leading edge and trailing edge have been specified as 15% and 20% of the chord length, respectively. The performance of the selected airfoil used the characteristic provided by [11] for higher supersonic region analysis. The present wing design is used as a baseline for further work where the wing geometry as well as wing composite structure is set as sensitivity parameter to obtain an optimum supersonic wing design.

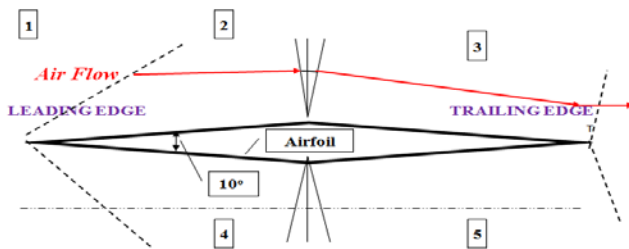


Fig. 1. Double Wedge Airfoil

For the external store, Figure 2 shows the configuration of the loaded missile on the wing. The external stores for each station of wing are specified in Table 1. There are two types of missiles used which are AMRAAM and Sidewinder.

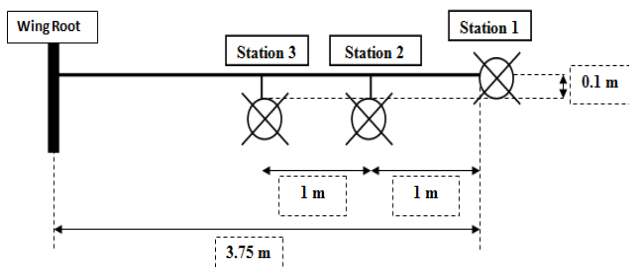


Fig. 2. External Stores Configuration On The Wing

Table 1. External Stores Technical Data

Station	Missile Type	Length (m)	Diameter (m)	Weight (kg)
1	AIM-9M	2.85	0.128	86.0
2	AIM-120 A	3.66	0.178	157.89
3	AIM-120 A	3.66	0.178	157.89

2.2. Wing Loading

Based on [3], the load factor for fighter aircraft is $n_z = 5.5$. The load for this wing, as shown in Fig.3, is assumed as an elliptic load acting along span wise; y-axis direction and symmetric quadratic load along chord wise; x-axis. With this load assumption, the sizing of the wing box can be conducted.

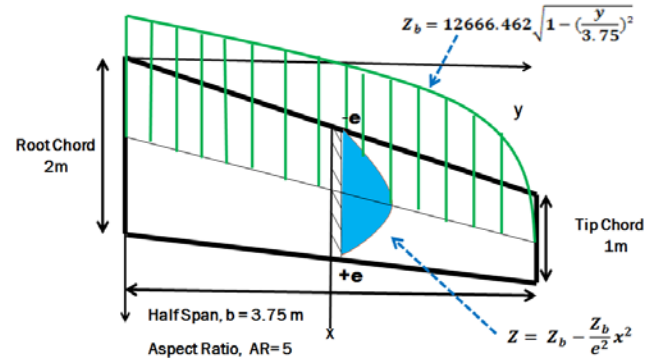


Fig. 3. Wing Loading Estimation Equation

The formula to calculate the load factor given by (1) in which L is the lift and W is the weight of the one side of the aircraft wing based on [11];

$$n_z = \frac{L}{W} \tag{1}$$

In which the lift can be calculated using (1)

$$L = n_z W \tag{2}$$

The span wise elliptic load can be formulated as

$$\left(\frac{y}{a}\right)^2 + \left(\frac{z_b}{b}\right)^2 = 1 \tag{3}$$

Where value of a is the half span length since it is minor axis length of the elliptic equation and b is the major axis length of the elliptic equation. Value of b can be calculated using (6). While for the chord wise quadratic load distribution:

$$z = C_0 + C_1x + C_2x^2 \tag{4}$$

The area of the quadratic load in chord wise direction can be calculated by integrating (4) acting along x axis.

$$A_{\text{quadratic}} = \int_{-c}^c z_b \left[1 - \left(\frac{x}{c}\right)^2\right] dx \tag{5}$$

Then, the volume of the elliptic load can be found by integrating (5) along y axis in (3)

$$V = \frac{4}{3} \int_0^a z_b(y) e(y) dy \tag{6}$$

To find the minor axis of elliptic equation in (3), equation (2) is divided by 2 since only applicable for half wing equal to the volume found in (3). This expression can be written as:

$$V = \frac{L}{2} \tag{7}$$

The wing can be assumed as a beam along y axis to find the shear stress of cutting section which is denoted in (8) and moment of cutting section which denoted in (9).

$$Q(y) = \int dQ \quad (8)$$

$$M(y) = \int dM \quad (9)$$

2.3. Skin Thickness

To calculate the skin thickness of the overall wing, the wing is divided into 4 regions along the span and calculated based on the load taken at that regions as shown in Fig. 4 and Fig. 5.

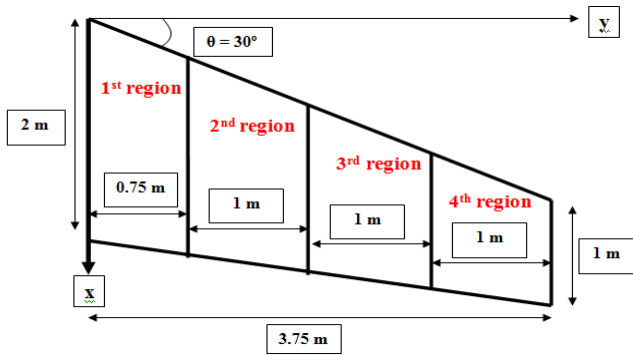


Fig. 4. Top View of Skin Thickness Division Region

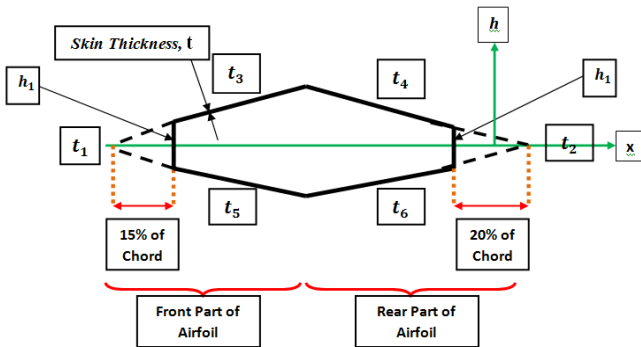


Fig. 5. Skin Thickness Segment in a Region

The moment of inertia formula is given as:

$$I = \int h^2 dA \quad (10)$$

The moment of inertia for the front and rear spar calculated as vertical segment as in (11)

$$I_{xx} = \frac{1}{12} th^3 \quad (11)$$

To determine the moment of inertia for any segment which has an inclination angle of θ , it can be derived using (10). This can be done using by setting the limit for integration along z axis from starting point in x, 0 to the end of each inclination segment denoted as b' . The final formula can be found in (12)

$$I = \frac{t}{\cos\theta} \int_0^{b'} \left(\frac{h}{2} + x \tan\theta \right)^2 \quad (12)$$

By assuming the thickness is same at every skin and spar, this will reduce to form an equation to find the thickness at any region based on the moment acting at that region where M is the moment at that region calculated by (9), h_{middle} is the height of the inclination only for front part of the wing and $I(t)$ is the summation moment of inertia of the wing box in term of t as the consistent thickness on at that selected region.

$$\sigma_y = \frac{M h_{middle}}{I(t)} \quad (13)$$

2.4. Factor of Safety

To ensure the safety of the wing box designed, Safety Factor, denoted as F.S is set at 1.5. The shear stress at location of any region in y direction denoted as τ_y is calculated using (14) with Q is the shear force at that region calculated using (8) in 2.2. , S is the summation of segment area multiply with the distance measured in z direction from the center of gravity, b^* is the summation of front spar and rear spar thickness and I is the summation of moment of inertia by substitution of the thickness value as in (11) and (12). The F.S then can be calculated using (15 α) or (15 β).

$$\tau_y = \frac{QS}{b^* I} \quad (14)$$

$$\frac{\tau_y}{\tau_{allow}} \leq F.S \quad (15\alpha)$$

$$\frac{\sigma_y}{\sigma_{allow}} \leq F.S \quad (15\beta)$$

3. UNSTEADY AERODYNAMICS

For the flutter prediction, unsteady aerodynamics acting on the wing surface, which is oscillating according to the structural dynamic mode shapes, is estimated using the boundary element method. For subsonic region, the unsteady aerodynamic is calculated using the doublet lattice method (DLM). While for supersonic region, a constant pressure method of ZONA51 is used. For both methods, the wing is modeled as flat lifting surface and is discretized into a number of trapezoidal elements.

Following [10], a set of aerodynamics influence coefficients in the form of matrix equation is generated. The fundamental relationships between the lifting pressure and the dimensionless normal velocity induced by the inclination of the surface to the air stream can be formulated as [10]:

$$\{w_j\} = [A_{ij}] \{f_j/q\}. \quad (16)$$

Where w is the normal wash velocity, f is the aerodynamic pressure, q is the dynamic pressure and A is the aerodynamic influence coefficient matrix. The substantial differentiation matrix of the structural deflections to obtain the downwash as in (17)

$$\{w_j\} = [D_{jk}^{1+i} k D_{jk}^2] \{u_k\} + \{w_j^g\} \quad (17)$$

where k is the reduced frequency. The integration of the pressure to obtain forces and moments,

$$\{P_k\} = [S_{kj}] \{f_r\} \tag{18}$$

The three matrices of (16), (17) and (18) can be combined and give the aerodynamics influence coefficient matrix in (19)

$$[Q_{kk}] = [S_{kj}] [A_{ij}]^{-1} [D_{jk}^1 + i k D_{jk}^2] \tag{19}$$

The ZONA51 and DLM theories compute the A matrix. Then, the matrix decomposition forward and backward substitutions are used in the computation of the Q matrix. Since this wing will be operating at supersonic region, the ZONA51 of Nastran had been used. For this part, the Nastran coding development in view of aerodynamics will consider the outer part of the wing box structure including the control surface as shown in Fig. 1.

4. PK METHOD OF FLUTTER SOLUTION

The PK equation for modal flutter analysis can be formulated as in (20)

$$\left[M_{hh} p^2 + \left(B_{hh} - \frac{1}{4} \rho c V Q_{hh}^1 \right) p + \left(k_{hh} - \frac{1}{2} \rho V^2 Q_{hh}^R \right) \right] \{u_h\} = 0 \tag{20}$$

where the circular frequency ω and the reduced frequency k are related to p as

$$k = \omega c / 2V \tag{21}$$

$$p = \omega (2g + i) \tag{22}$$

The flutter solution is rewritten in the state space form as in (23) where A is in complex numbers.

$$[A - p I] \{u_h\} = 0 \tag{23}$$

The Eigen solutions to (23) is in the form of a complex number Eigen value p for each mode, which in turn will give the structural damping g for the real part and frequency ω for the imaginary part. Note that the result is computed for each velocity which is embedded in the damping and stiffness term of Eq. (20).

5. RESULTS

5.1. Normal Modes – SOL 103 of MSC Nastran

For the FEM data, boundary condition at the wing root is set to be zero deflection and rotation in x, y, z direction at the front, middle and rear spars of the wing box. The first 8 normal modes of the wing structure are shown in Fig. 6 until Fig. 13. Note that the rigid body mode is not included in the list. The frequency and its associated shape are recorded in Table 2.

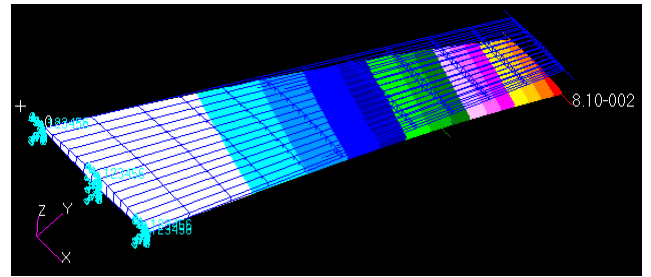


Fig. 6. Mode 1

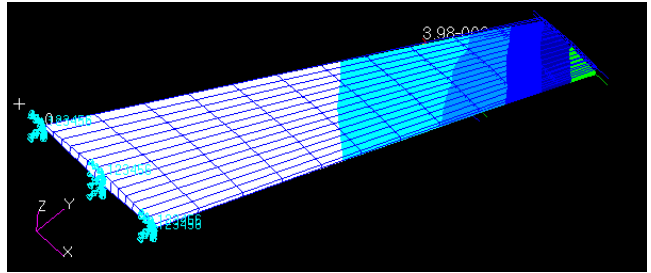


Fig. 7. Mode 2

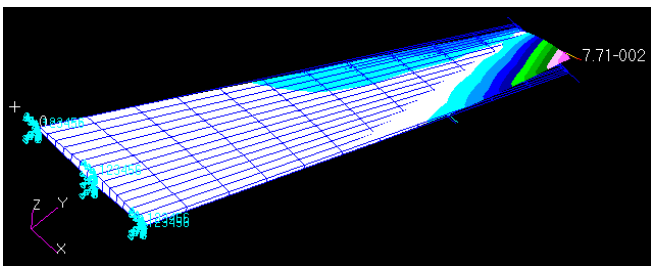


Fig. 8. Mode 3

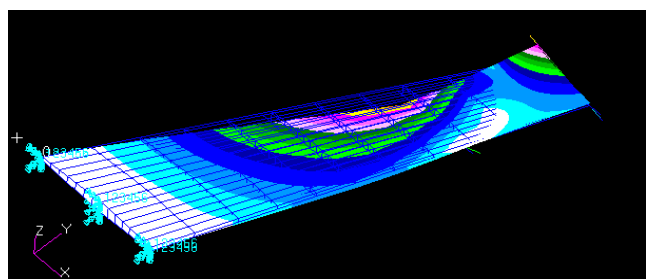


Fig. 9. Mode 4

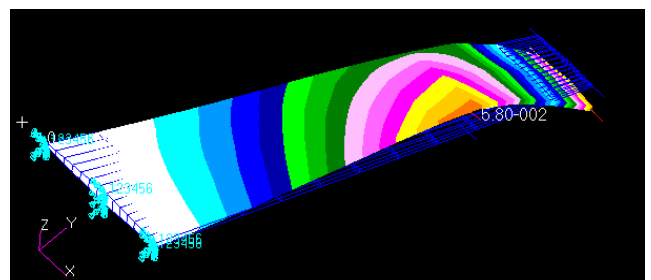


Fig. 10. Mode 5

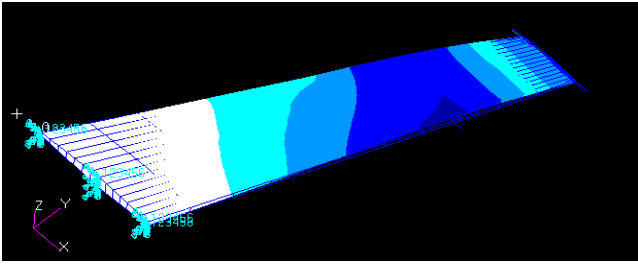


Fig. 11. Mode 6

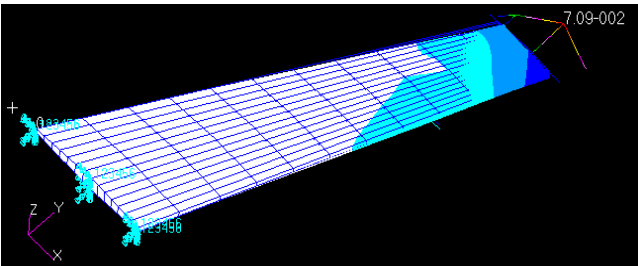


Fig. 12. Mode 7

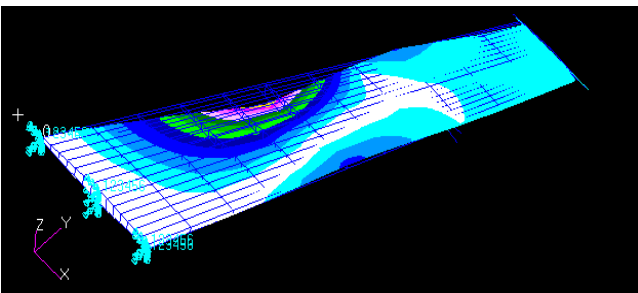


Fig. 13. Mode 8

Table 2. Normal Modes Data

MODE	Frequency (Hz)	Description of Modes
1	3.7911	Pure Bending
2	5.2694	Mix Torsion and Bending
3	6.1196	Torsion
4	9.3154	Torsion
5	11.929	Torsion
6	13.656	Torsion
7	16.687	Mix Torsion and Bending
8	17.602	Torsion

5.2. Flutter Solution – Sol 145 of MSC Nastran

The simulation undergoes further solution called SOL 145. This solution had been simulated at different Mach number to find the match point velocity at 0 ft (sea level). The graph of structural damping versus velocity of every mode at 0 ft is plotted in Fig. 14. Besides that, a graph of velocity versus frequency at 0 ft in Fig. 17 also plotted to show the rapid changes of frequency of the flutter mode.

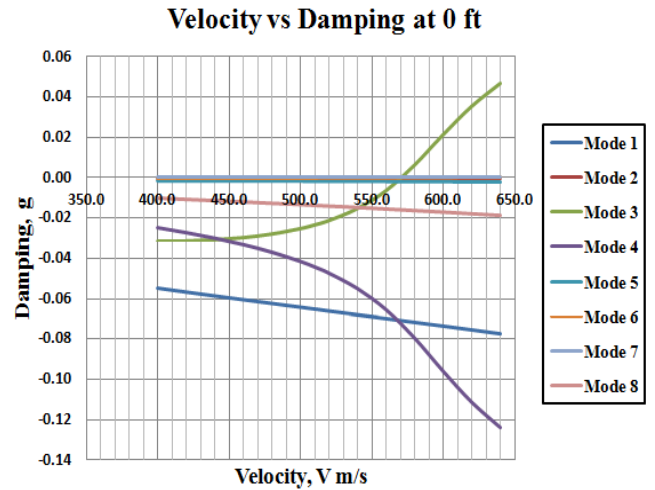


Fig. 14 Graph of Velocity vs. Damping at 0 ft

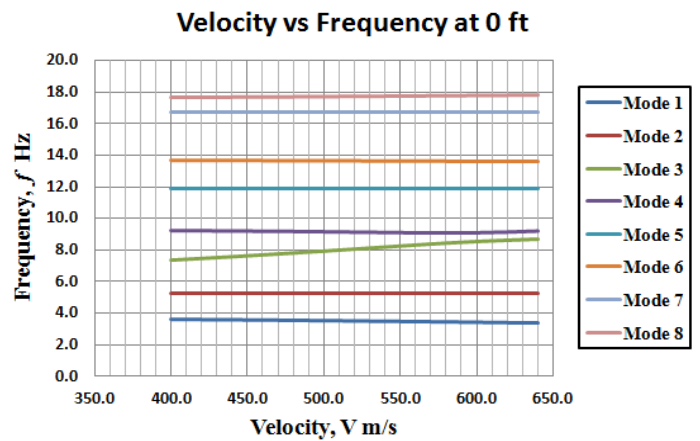


Fig. 15 Graph of Velocity vs. Frequency at 0 ft

The flutter mode most likely occurs at Mode 3 since the graph in Fig. 14 show that the structural damping become zero when it approximately approaching velocity at 570 m/s. This is the match point for the graph since at this speed it gives the result of Mach number 1.67. The simulation for this solution repeated for different altitudes. The graphical figure in Fig. 18 shows the variation of flutter speed of this mode. The flutter velocity and flutter Mach number for this variation shows in Table 3. The result shows that the present wing flutter is sensitive to the altitude. For this reason, the calculation is performed also to a negative altitude where $h_{neg} = - 7,943$ ft. This negative altitude is derived analytically in [12] for transport aircraft and military UAV (Unmanned Air Vehicle)

which is, according to Standard Regulation of [13], defined as the altitude as the result of all combinations of altitudes and speeds encompassed by the V_{Dive} or M_{Dive} versus altitude envelope enlarged at all points by an increase of 15 percent in equivalent airspeed at both constant Mach number and constant altitude.

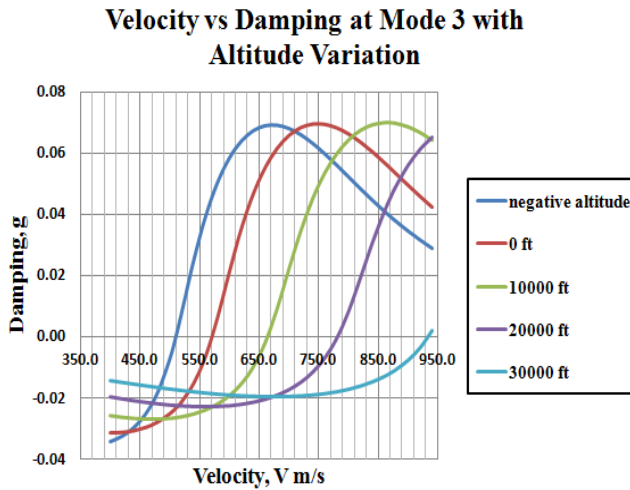


Fig. 16. Graph of Velocity vs Damping at Different Altitude for Mode 3

Table 3. Flutter Velocity and Flutter Mach Number

Altitude (ft)	Flutter Velocity (m/s)	Flutter Mach Number	Flutter Frequency (Hz)
-7943	490	1.40	8.35
0	570	1.67	8.36
10000	670	2.04	8.40
20000	790	2.50	8.45
30000	930	3.08	8.40

6. CONCLUSION

The present work established a procedure for the wing design based on flutter analysis. The external stores give a significant effect on the wing flutter. The result also showed that the present wing-external store flutter is sensitive to the flight altitude. The present result is used as baseline for further work where an aeroelastic tailoring to find optimum composite structure for the main wing box is conducted in order to find higher flutter speed and lighter wing structure.

ACKNOWLEDGMENT

Special thanks to the Science and Technology Research Institute for Defense (STRIDE) Malaysia for allowing the present authors to use MSC Nastran and MSC Patran in their

facilities. The present research is funded under IIUM Research Endowment Fund EDW B11-178-0656.

REFERENCES

- [1] MSC, "MSC Developments in Aeroelasticity". Aerospace Users' Conference Proceedings Los Angeles, California: The MacNeal-Schwendler Corporation, (p. 2), 1997.
- [2] J. R. Wright, and J. E. Cooper, Aircraft Aeroelasticity and Loads, Manchester, United Kingdom: Jon Wiley & Sons Ltd, 2007.
- [3] MIL-A-M8861B(A). Military Specification :Airplane Strength and Rigidity Flight Loads. Lakehurst, New Jersey: Naval Air Engineering Center, Systems Engineering and Standardization, 1986.
- [4] MIL-A-8870C(AS). Military Specification: Airplane Strength and Rigidity Vibration, Flutter, Divergence. Lakehurst, New Jersey: Commanding Officer, Naval Air Warfare Center Aircraft Division, 1993.
- [5] B. Peeters, H. Climent, R. d. Diego, J. d. Alba, J. R. Ahlquist, J. M. Carreño et al. "Modern solutions for Ground Vibration Testing of large aircraft". Proceeding of IMAC 26, Orlando , USA, p. 2, 2008.
- [6] D. P. Raymer, Aircraft Design : A Conceptual Approach. Reston: American Institute of Aeronautics and Astronautics, Inc, 1999.
- [7] S. Janardhan, R. V. Grandhi, F. Eastep, & B. Sanders, "Parametric Studies of Transonic Flutter and Limit-Cycle Oscillation of an Aircraft Wing/Tip store". Journal of Aircraft , p. 20, 2003.
- [8] Approved Navy Training System Plan For The AIM-120 Advanced Medium Range Air to Air Missile. Nevada: Naval Strike and Air Warfare Center (NSAWC), 1988.
- [9] AIM -9 Sidewinder. (n.d.). Retrieved from Operation Guide: www.vojenskeletectvi.cz
- [10] MSC Nastran. MSC.Nastran Version 68. In Aeroelastic Analysis User's Guide. MSC.Software Corporation.
- [11] E. D. Motte, "Gripen : When logic is part of the equation" Farnborough, UK: Gripen Export, Saab Aeronautics, 2012.
- [12] E. Sulaeman, "On the Evaluation of Negative Altitude Requirement for Flutter Speed Boundary of Transport Aircraft and UAV", Applied Mechanics and Materials, Vol. 225, pp. 397-202, 2012, ISBN: 13 978-3-03785-506-5.
- [13] UAV Systems Airworthiness Requirements (USAR) for North Atlantic Treaty Organization (NATO) Military UAV Systems – Standard Agreement STANAG 4671 (Edition 1), 2009.
- [14] K. H. Yu, H. Djojodihardjo, & H. Kadarman "Acoustic Effects On Binary Aeroelasticity Model". IIUM Engineering Journal, Vol. 12, No. 2 , pp. 123-126, 2011